Journal of Building Engineering 103 (2025) 112115

Contents lists available at ScienceDirect

Journal of Building Engineering

journal homepage: www.elsevier.com/locate/jobe

Impact of electrical heating on carbon textile reinforced concrete under freeze-thaw exposure

Annette Dahlhoff *, Michael Raupach

Institute of Building Materials Research (ibac), RWTH Aachen University, Schinkelstr. 3, 52062, Aachen, Germany

ARTICLE INFO

Keywords:
Carbon textile reinforced concrete
Electrical heating
Freeze-thaw
Tensile strength test
Crack distribution

ABSTRACT

Carbon textile reinforced concrete (CTRC) is increasingly used as a high-performance composite material in the construction industry, combining concrete with non-metallic reinforcement. Characterized by remarkable material properties such as tensile strength, durability, and density, CTRC also features high electrical conductivity, which enables electrical heat generation within building components. This paper assesses the potential of ice-prevention using electrically heated CTRC in building constructions. To quantify the effects of various material parameters, tensile strength tests were conducted after freeze-thaw exposure of carbon textile reinforcements (CTR), which were impregnated with epoxy resin and surface-modified with quartz sand, as well as the composite CTRC. The findings were compared with those of electrically heated CTRC exposed to freeze-thaw cycles with active electrical heating throughout the frost period. The study presents pioneering findings, demonstrating that electrical heating effectively prevents the freezing of CTRC at sub-zero temperatures, with no adverse impacts on tensile strength or crack distribution. This research combines material research with thermal performance, offering important insights into the practical applications of CTR in innovative building designs.

1. Introduction

The composite material carbon textile reinforced concrete, referred to as CTRC, is an innovative construction material consisting of a high-performance carbon textile reinforcement embedded in a fine-grain mortar matrix. This combination enables thin, durable and resource-efficient structures with outstanding material properties, such as tensile strength of up to 4200 N/mm^2 [1–3]. Additionally, the carbon fibers are electrically conductive. In this context, the electrical and high thermal conductivity of carbon fibers along the fiber direction can be utilized for the development of electrically heated carbon textile reinforced concrete, cf. Fig. 1 [4,5]. This innovative multifunctional technique can be employed as a heating element in building components by utilizing Joule's heating principle [6]. The temperature rises as an electrical voltage is applied to the conductor, generating heat [7].

Building materials research has analyzed various potential applications, examining how this electrical heating technology can be effectively utilized in construction. For example, CTRC can function as an electrical resistance heating element, offering capabilities such as radiant heating or heat storage in concrete components, and thus providing protection against condensation [8,9]. This was demonstrated by implementing electrically heated CTRC as radiant heating in wall components [10,11]. Additionally, the heat generated by the electrically heated CTRC positively affected the hydration process of the concrete and can be used for de-icing outdoor facilities, such as parking lots, airport infrastructure and bridges [12,13]. Xu et al. [14] have conducted both numerical

* Corresponding author.
E-mail address: dahlhoff@ibac.rwth-aachen.de (A. Dahlhoff).

https://doi.org/10.1016/j.jobe.2025.112115
Received 7 October 2024; Received in revised form 23 January 2025; Accepted 11 February 2025
Available online 14 February 2025

and experimental investigations into the electrothermal properties. Their research has validated the potential for de-icing through the heat generated in carbon/glass fiber hybrid textile reinforced concrete [14].

The potential for ice-preventing was further investigated by exposing test specimens to freeze-thaw exposure in this study. Test series with electrical heating were compared to unheated reference series under these conditions to analyze the effects on mechanical properties. In the test series with electrical heating, the temperature control system activates the heating to keep the test specimen's temperature above 0 °C, preventing them from freezing, cf. Fig. 2.

To effectively implement the proposed use of electrically heated CTRC for deicing, it is essential to investigate the material's behavior under freeze-thaw temperature conditions. To contextualize the behavior of electrically heated CTRC and the results of this study, findings related to frost attack on the mechanical performance of CTRC are summarized, cf. Table 1. This summary focuses specifically on studies using carbon as fiber material.

Arboleda et al. [16] conducted experimental tests to investigate the durability characteristics of two fabric reinforced cementitious matrix composites, one with carbon fiber fabric and the other with polyparaphenylene benzobisoxazole (PBO) fiber fabric. The study evaluated the impact of environmental conditions, including frost and chemical attack, by exposing the materials to freeze-thaw cycles. No significant degradation was observed in the environments studied. Arboleda et al. [16] assumed that the increased strength observed after 28 days resulted from continued hydration. Furthermore, Yin et al. [17] investigated a hybrid fiber material composed of carbon and e-glass, with an additional sand coating. As the number of chloride freeze-thaw cycles increased, the average interfacial bonding strength between the fiber yarn and fine-grained concrete decreased. The reduction in bonding strength became more pronounced after 90 freeze-thaw cycles. The interaction between chloride freeze-thaw cycles and long-term exposure accelerated the deterioration of flexural properties, with increasing deterioration as the duration of loading extended [17]. As an additional application area, Tedeschi [19] examined the material combination in the context of masonry strengthening. The results showed that thermal aging caused irreversible damage due to the differing behavior of the matrixes, particularly with weak and high porous bricks found in historical contexts [19]. Additionally, Heins et al. [2] investigated the long-term bonding and tensile strength of CTR mortar under freeze-thaw and hot weather environments. Although up to 300 cycles were tested for each condition, no significant degradation was observed in the specimens. The tensile strength of the specimens conditioned for up to 300 cycles under freeze-thaw and hot weather conditions was at least 90 % compared to the unconditioned specimens. Therefore, Heins et al. [2] assumed that freeze-thaw and high temperatures may not be significant factors affecting the degradation of CTRC with surface-coated textiles [2]. Furthermore Sheng et al. [20] conducted additional experiments to evaluate the mechanical performance of CTRC-strengthened beams in salt freeze-thaw environment. Sheng et al. [20] analyzed the effects of freeze-thaw cycles, installation methods, as well as sustained loading on the failure modes, crack patterns, load-deflection behavior, and bearing capacity of the beams. The results showed resistance to freeze-thaw exposure, with only minimal cement paste peeling off the specimens' surface after 60 cycles. However, the ultimate load of the beams decreased linearly as the number of freeze-thaw cycles increased. Moreover, the ultimate load decreased due to the combined effects of freeze-thaw cycles with increasing sustained loading [20]. Furthermore, Shiping et al. [21] investigated the effects of various freeze-thaw environments, cycles, textile layers and types, as well as textile coatings. The results demonstrated that specimens exposed to freeze-thaw cycles in chloride salt exhibited increased the tensile strength compared to those in sulfate solutions, while specimens in clear water showed relatively lower tensile strength. As the number of freeze-thaw cycles increased, both ultimate tensile strength and flexural performance of the specimens decreased. In terms of textile layers, double-layer textile specimens showed improved stiffness and bearing capacity under freeze-thaw conditions compared to single-layer specimens, through their deformation capacity was decreased. In addition, a reduction in tensile strength and flexural performance was indicated for basalt-glass textile specimens compared to carbon-glass textiles. On the other hand, carbon-glass textiles impregnated with epoxy resin and covered with sand exhibited decreased ultimate tensile strength and bending stress [21]. The summarized literature results on tensile strength after freeze-thaw exposure, represented as the reduction factor K_{FT} relative to tensile strength without freeze-thaw exposure, are depicted in Fig. 3.

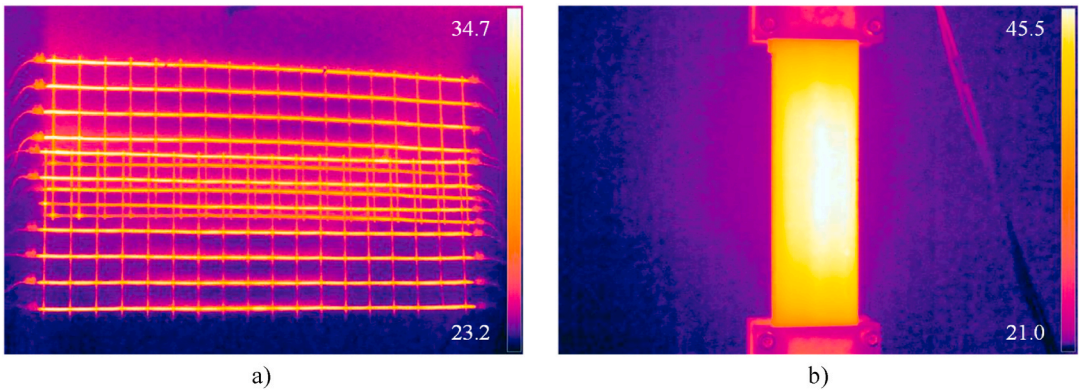

Fig. 1. Exemplarily heated CTR and CTRC captured with a thermal imaging camera: a) Acrylate-impregnated CTR – weft fiber strand connected; b) Heated CTRC tensile specimens.

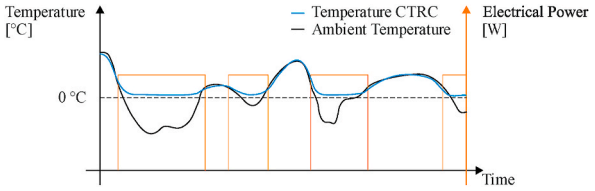

Fig. 2. Potential for ice-prevention through temperature regulation using electrically heated CTRC.

Table 1
Overview of literature on frost attack with freeze-thaw exposure [2,15–22].

Reference	Fibre Material	Matrix Material	Standard	Conditions	Duration	Post-Exposed Test
Micelli et al. [15]	carbon	–	ASTM C666-92	−18 °C ↔ 4 °C; followed by high temperature cycle 16 °C ↔ 49 °C	200 cycles	Tensile strength test
Arboleda et al. [16]	carbon and PBO	mortar	AC434	−18 °C↔ 37.7 °C; 100 % RH	20 cycles: 4 h freezing, 12 h thawing	tensile strength test; adhesion test
Yin et al. [17]	hybrid (carbon and e-glass with sand)	fine grained concrete	GB/T 50082-2009	−18 °C ↔ 5 °C; with saline [5 % NaCl]	50/70/90 cycles: 3 h freezing, 3 h thawing	pull-out and flexural
Nobili et al. [18]	carbon	mortar	AC434	−18 °C↔ 37.7 °C; 100 % RH	20 cycles: 4 h freezing, 12 h thawing	tensile strength test
Tedeschi et al. [19]	carbon	mortar	–	−10 °C ↔ 70 °C; 60 % RH	40 cycles: 3 h freezing, 3 h thawing	pull off
Heins et al. [2]	carbon	mortar	–	−18 °C ↔ 4 °C	100/200/300 cycles: 3 h freezing, 3 h thawing	tensile strength test; pull-out test
Sheng et al. [20]	hybrid (carbon and e-glass)	fine grained concrete	GB/T 50082-2009	−18 °C ↔ 5 °C; with saline [5 % NaCl]	60 cycles: 3 h freezing, 3 h thawing	four-point bending test
Shiping et al. [21]	hybrid (carbon and AR-glass; basalt and AR-glass; carbon and AR-glass with EP and covered sand)	fine grained concrete	–	N/A	50/75/100 cycles	tensile strength test; four-point bending test

RH: relative humidity.
PBO: polyparaphenylene benzobisoxazole.
EP: epoxy resin.
N/A: not available.

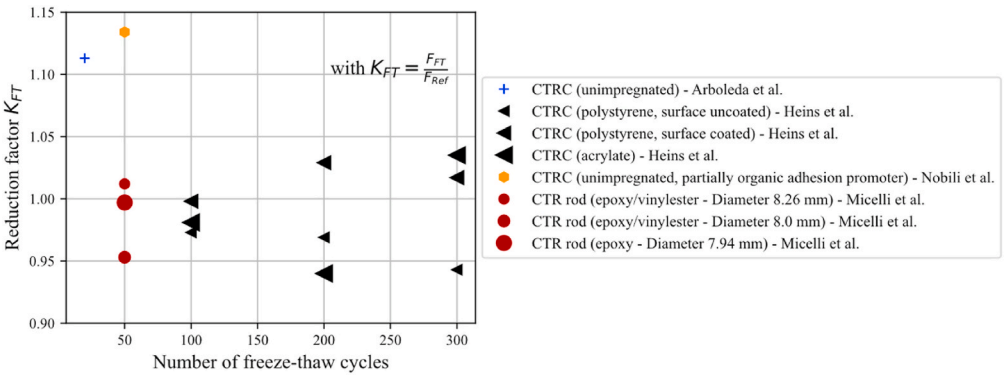

Fig. 3. Results from literature on the frost attack for the reduction factor K_{FT} related to the tensile strength of reference conditions [2,15,16,18].

$$K_{FT} = F_{FT} / F_{Ref} \quad (1)$$

with:

K_{FT} being the reduction factor;
F_{FT} being the tensile strength after freeze-thaw exposure in N/mm^2;
F_{Ref} being the tensile strength without freeze-thaw exposure as the reference in N/mm^2.

Alma'aitah et al. [22] summarized the literature findings on frost attack in their review. Freeze-thaw conditions can significantly impact CTRC by degrading the matrix, reducing its cracking strength, deteriorating the bond between the textile and matrix, and potentially damaging the textile itself, depending on the coating used. The extent of this deterioration is influenced by factors such as the strength of the matrix, the textile-to-matrix bond, boundary conditions, and exposure factors like temperature, number of cycles and degree of saturation. Alma'aitah et al. [22] described that a notable issue is the absence of standardized protocols for evaluation the freeze-thaw resistance of textile reinforced concrete composites, leading researchers to use various testing methods and cycle counts. This lack complicates comparisons between different experimental results. Summarizing the results from literature, experimental studies reported improvements in tensile behavior under freeze-thaw conditions, potentially due to matrix hydration, others have examined reductions in cracking load, tensile strength, or flexural strength. Research on the textile-to-matrix bond interaction examined no clear trend [22].

To assess the potential of de-icing with electrically heated CTR in construction materials, especially their performance in freeze-thaw environments, experimental tests were conducted using CTRC tensile specimens. In contrast to the existing literature, which mainly discusses material properties related to frost attack, this paper specifically investigates the tensile load-bearing behavior and crack performance of CTR and electrically heated CTRC in freeze-thaw environment.

2. Materials

In this study, a carbon textile reinforced composite, composed of a commercially available carbon textile reinforcement (CTR) and a repair mortar, according to Refs. [23,24], was used for the evaluation. The examined CTR was impregnated with epoxy resin and additionally, surface modified. The surface modification included an additional coating of epoxy resin and quartz sand. The investigated CTR is referred to as CTR-EP-Sand. The CTR-EP-Sand consists of a rectangular roving axis distance of 21 mm and an equal roving cross-section of 0.90 mm^2 in both the warp and weft directions [25]. The investigated carbon textile reinforcement CTR-EP-Sand is shown in Fig. 4, and the material parameters are summarized in Table 2.

For the investigation of the composite, a polymer-modified cement-based mortar designed for repairing and retrofitting concrete surfaces, with a maximum grain size of 2 mm was used, as described in Refs. [23,24]. The material properties of the mortar are presented in Table 3. According to manufactures' declaration of performance, the mortar exhibits high resistance to freeze-thaw exposure [26].

3. Experimental investigation

3.1. Testing programme

In this study, the material behavior of the presented reinforcement material and composite under freeze-thaw cycling was investigated through experimental tests on the carbon textile reinforcement (CTR) and carbon textile reinforced concrete (CTRC). The

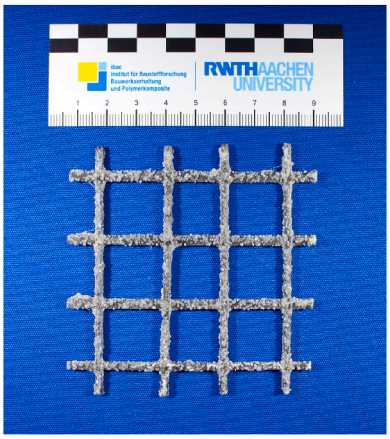

Fig. 4. Investigated carbon textile reinforcement – CTR-EP-Sand.

Table 2
Material parameters of the carbon textile reinforcement according to the manufacturer's specification [25].

Reinforcement	Roving Axis Distance longitudinal/transversal	Roving Cross-Section	Textile Cross-Section	Titer	Average Tensile Strength (Wrap Direction)
[−]	[mm]	[mm^2]	[mm^2/m]	[tex]	[MPa]
CTR-EP-Sand	21/21	0.90/0.90	43/43	1600/1600	4200 ± 215 [1)]

[1] Measurements performed at the Institute of Building Materials Research (IBAC), RWTH Aachen University.

Table 3
Material parameters of the repair mortar.

Mortar	Compressive Strength [1)]	Bending Strength [1)]
[−]	[MPa]	[MPa]
RM-A4	68 ± 3	11.5 ± 1.1

[1] Measurements performed at the Institute of Building Materials Research (IBAC), RWTH Aachen University after 28 days.

initial test series focused on the CTR, which included roving specimens subjected to freeze-thaw cycling, referred to as CTR-FT, and reference specimens that were not exposed to freeze-thaw exposure, referred to as CTR-Ref. The subsequent test series examined the composite carbon textile reinforced concrete, categorized as follows: CTRC-FT, exposed to freeze-thaw cycling; CTRC-FT-c, pre-cracked specimens of the composite exposed to freeze-thaw cycling; CTRC-FT-e-c, electrically heated and pre-cracked specimens subjected to freeze-thaw cycling; CTRC-FT-e, electrically heated specimens also exposed to freeze-thaw cycling; and CTRC-Ref, reference specimens not subjected to freeze-thaw cycling.

In the test series with electrical heating, the temperature control activates the heating to keep the test specimen's temperature above 0 °C, thereby preventing freezing, cf. Fig. 2.

To evaluate the material behavior, the mass change was investigated throughout the freeze-thaw cycles at 7-day intervals. Additionally, microscopic examinations were performed at 7-day intervals during the cycling to analyze changes in cracks. Finally, tensile strength tests were conducted after the 28-day freeze-thaw exposure. These tests included roving tensile tests for the CTR and tensile specimen tests for the CTRC, providing a thorough assessment of the materials' performance and durability under simulated environmental conditions. The experimental test process and test series are summarized in Fig. 5 and Table 4.

3.2. Experimental setup and testing procedure

The experimental setup and testing procedure are subdivided into two main parts. The initial part examined tensile strength tests on the individual CTR, followed by experiments on the CTRC.

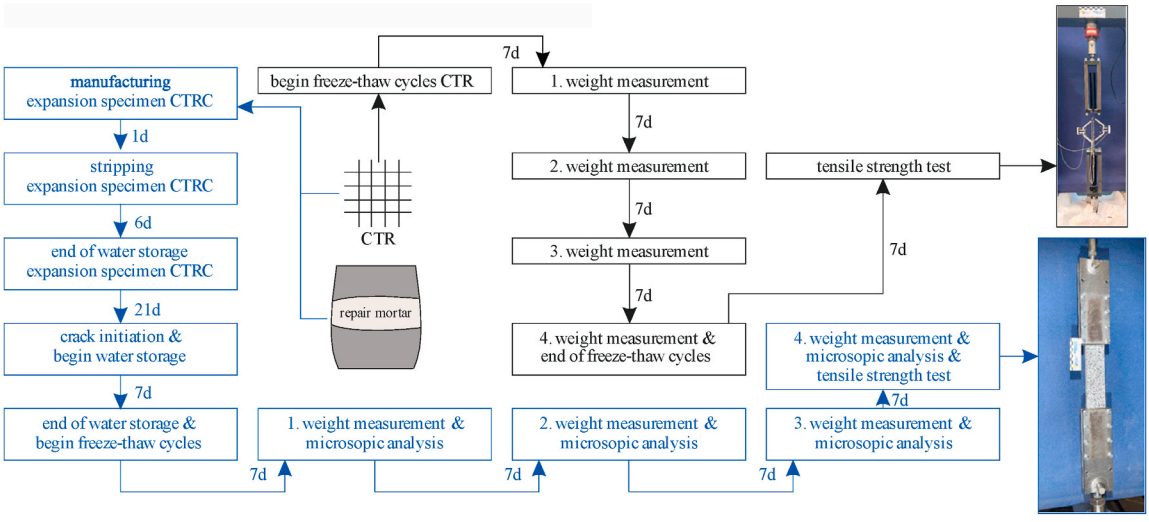

Fig. 5. Overview of the experimental test process.

Table 4
Overview of the investigated experimental test series.

Test Series		Experimental Test		
		Mass Change	Microscopy	Tensile Strength Test
		Test dates (No. of Specimens) [2)]	Test dates (No. of Specimens) [2)]	Test dates (No. of Specimens) [2)]
CTR	CTR-FT	0/7/14/28 d (1)	–	28 d (10)
	CTR-Ref	0/7/14/28 d (1)	–	28 d (10)
CTRC[1)]	CTRC-FT	0/7/14/28 d (3)	–	28 d (3)
	CTRC-FT-c	0/7/14/28 d (3)	0/7/14/28 d (3)	28 d (3)
	CTRC-FT-e-c	0/7/14/28 d (3)	0/7/14/28 d (3)	28 d (3)
	CTRC-FT-e	0/7/14/28 d (3)	–	28 d (3)
	CTRC-Ref	0/7/14/28 d (3)	–	28 d (3)

FT = Freezing Thaw Exposure; c = pre-cracked after 28 days of manufacturing; Ref = Reference; e = electrically heated CTR.
[1] CTR-EP-Sand in combination with RM-A4.
[2] Test dates relative to the start of freeze-thaw cycling in days.

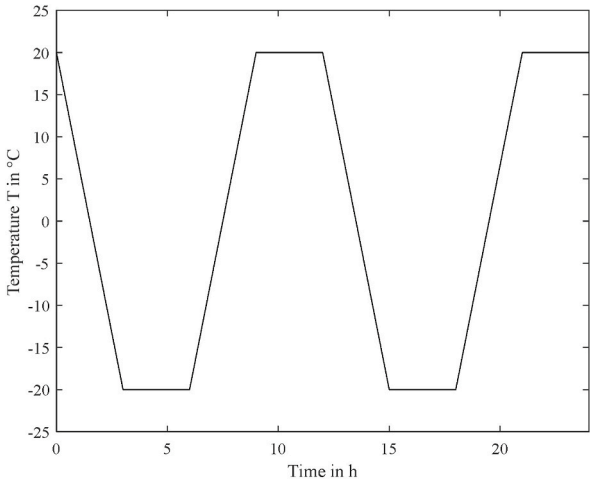

Fig. 6. Temperature profile of the freeze-thaw cycle.

3.2.1. CTR testing - tensile strength tests and mass change analysis

To investigate the impact of freeze-thaw exposure on the material behavior of CTR, tensile strength tests were conducted and mass changes were analyzed on commercially available fiber strands (FS). Since commercially available FS were used, a separate analysis of

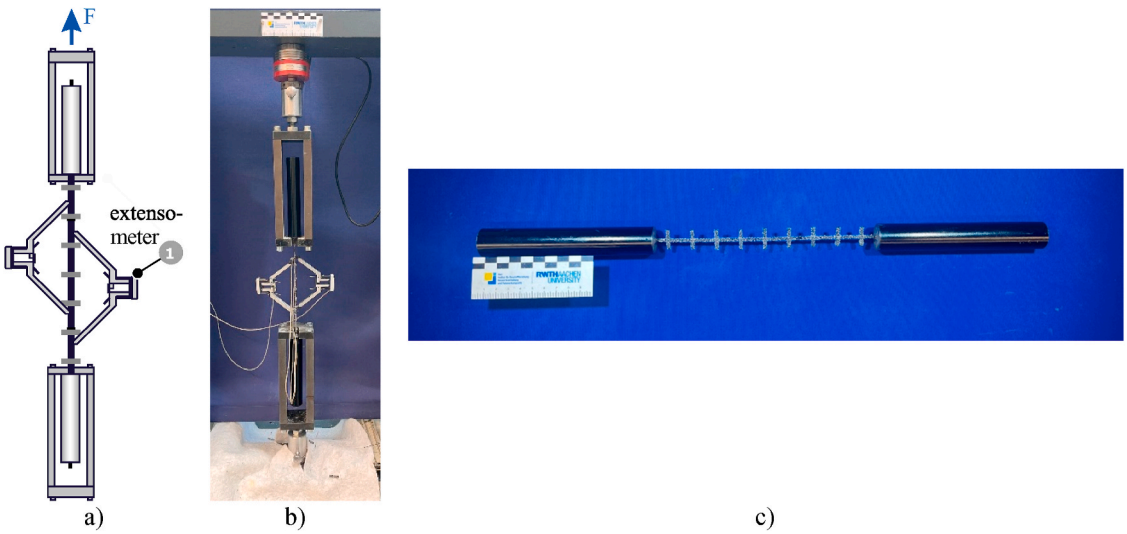

Fig. 7. FS tensile strength test setup: a) Schematically drawing; b) Overview of test setup; c) Exemplarily fiber strand CTR-Ref.

impregnation materials and coating was not performed.

For evaluating the freeze-thaw behavior of the CTR-FT, the reinforcement was placed in a climate chamber subjected to freeze-thaw cycling for 28 days. The cyclical temperature profile is shown in Fig. 6.

During the freeze-thaw-cycling, the specimen was weighed every 7 days, and the mass change was determined for CTR-FT. For comparison, the CTR-Ref specimen was stored at room temperature 23 ± 5 °C and weighed at the same 7-day intervals.

Following the temperature exposure, the FS were prepared for tensile strength testing. Specimens with a total length of 500 mm were cut from the textile reinforcement grid in the wrap direction and cast into 150 mm-long steel hulls using grout mortar. After a 7-day curing period for the grout mortar, uniaxial tensile strength tests were performed using a Zwick ZMART.Pro universal testing machine with a 10 kN load cell, and a controlled testing speed of 2 mm/min, as depicted in Fig. 7. The load and the crosshead displacement were recorded in the TestXpert® software. During the test series, the deformation was measured with two extensometers, each with a gauge length of 100 mm, and the strain was calculated accordingly. The strain at the specimens' failure was analyzed based on the linear-elastic behavior of the CTR through linear regression on the stress-strain curve, using the determined tensile strength [1, 27,28]. Ten specimens were examined for each series, CTR-FT and CTR-Ref.

3.2.2. CTRC testing - tensile strength tests; microscopy and mass change analysis

To determine the material behavior of electrically heated CTRC exposed to freeze-thaw conditions, CTRC specimens were analyzed for tensile strength, mass change, and crack development. The specimens measured 500 x 60 × 20 mm³ (L x W x T) and were manufactured with a constant mortar cover of RM-A4 on both sides with a single layer of CTR, cf. Fig. 8. The specimens were hand-laminated using a solid to water weight ratio of 1:0.13. During the manufacturing process, the properties of the fresh mortar were evaluated according to Refs. [29–31], and standard prism sets were prepared to determine the flexural and compressive strength in accordance with [32] after 28 days.

After one day, the tensile specimens were stripped of the formwork and stored in water for 7 days. Afterwards, the specimens were stored at a temperature of 24 ± 8 °C and a relative humidity of 53 ± 23 % until the age of 28 days, respectively. In the test series CTRC-FT-e-c and CTRC-FT-c, cracks were initiated on day 28 after manufacturing. Preliminary tests were conducted to determine the loading required based on crack development in CTRC. The loading was selected to ensure that Stage IIa was fully completed, as shown in Fig. 9.

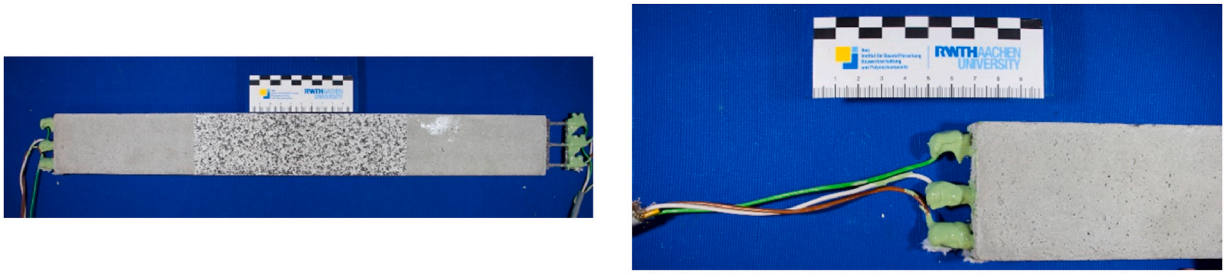

Fig. 8. Tensile specimens: a) CTRC tensile specimen with sprayed stochastic pattern; b) Detail of the connections.

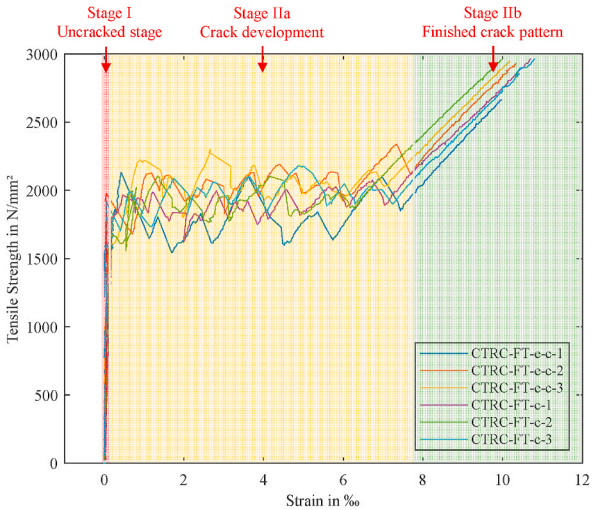

Fig. 9. Crack Initiation of CTRC tensile specimens.

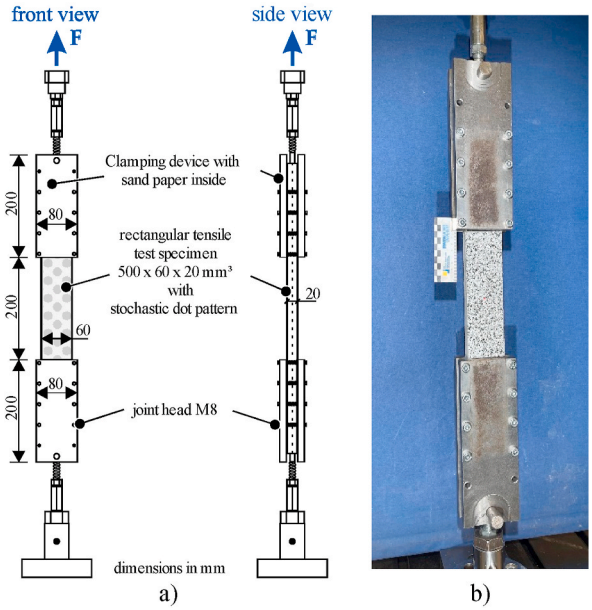

Fig. 10. Test setup for pre-cracking and tensile strength tests on CTRC specimens: a) Schematic drawing; b) Overview of test setup.

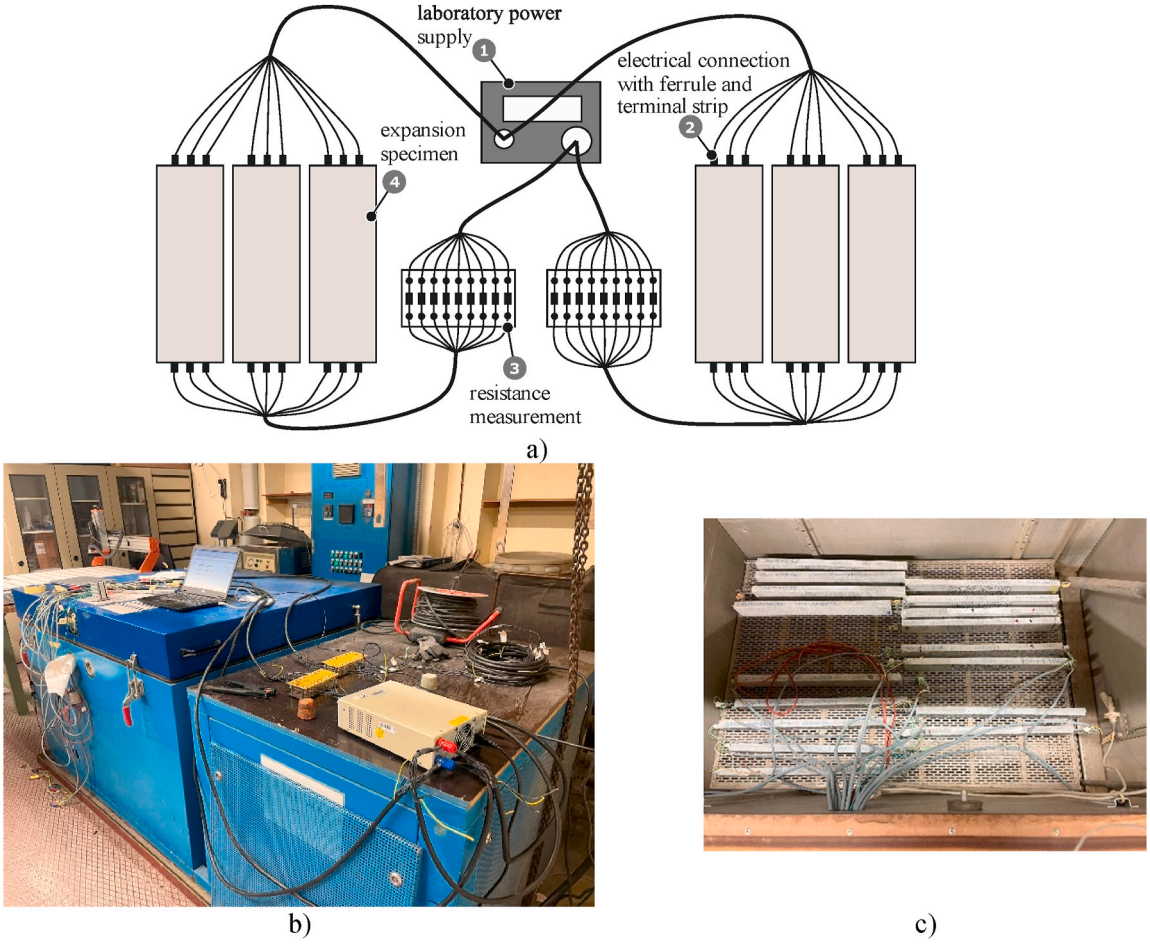

Fig. 11. Test setup for the freeze-thaw exposure: a) Technical drawing – circuit; b) Overview of climatic chamber; c) Overview of tensile specimen in climatic chamber.

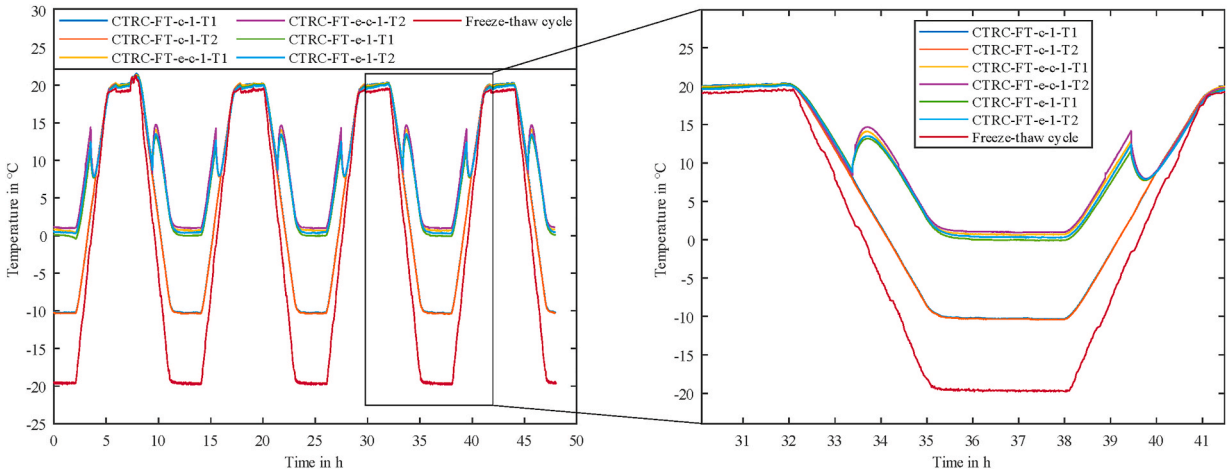

Fig. 12. Temperature profile of the tensile specimen and freeze-thaw cycle.

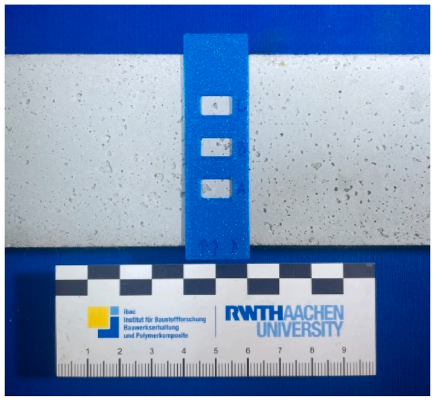

Fig. 13. Positioning tool for the microscopic analyzes.

For testing, the specimens were clamped between steel plates in the upper and lower load introduction areas over a length of 150 mm, as illustrated in Fig. 10 [7]. A torque of 25 Nm was applied. Crack initiation was performed using a 150 kN universal testing machine (Zwick Z150 TL) with a displacement control rate of 2 mm/min until reaching 3000 N/mm^2 load level. Load and crosshead displacement were recorded in the software TestXpert®.

To analyze the full-field deformation of the surface during testing, the optical 2D/3D measuring system ARAMIS® from GOM GmbH was employed. This contact-free system provides precise load- and time-dependent measurements of crack formation and development. A stochastic pattern was applied to the measurement area of the CTRC tensile specimens to facilitate this analysis. The system, equipped with 5M cameras, was calibrated with a measurement volume of 270 x 230 × 230 mm^3, a mean calibration deviation of 0.023 pixels, and a scale deviation of 0.001 pixels. For deformation analysis, 5 images per second were captured. According to the parameters established in Ref. [5], the facet size was set to 15 x 15 pixels, the pixel overlap to 3 pixels, and the threshold for major strain was defined as 0.5 %.

All CTRC specimens were stored in water for 7 days after 28 days of curing and then the CTRC-FT series subjected to freeze-thaw cycling for 28 days, as shown in Figs. 6 and 11. During the freeze period, the CTRC-FT-e-c and CTRC-FT-e specimens were electrically heated. For this, the ends of the specimens were connected using ferrules and terminal strips, and then linked to a laboratory power supply. To protect the connections from moisture damage in the climate simulation, a two-component epoxy coating was applied. The electrical power required to maintain the specimens above 0 °C was determined in preliminary tests in a climatic chamber. During the freeze period, the electrically heated specimens were subjected to a terminal voltage of 10 V, with a resulting current of 11 A. Fig. 12 shows the temperature profile measured with thermo elements in the electrically heated tensile specimens, in relation to the temperature curve of the freeze-thaw cycle. The CTRC-Ref Series was stored in a climate room at a temperature of 20 ± 1 °C and a relative humidity of 65 ± 10 % until testing at the age of 63 days, respectively.

During the freeze-thaw cycle, the masses of the tensile specimens were measured at 7-day intervals, and the initiated cracks were analyzed microscopically with 16× magnification. Fig. 13 depicts the positioning tool to examine the identical analysis position.

For testing, the specimens were clamped between steel plates in the upper and lower load introduction areas over a length of 150 mm, as illustrated in Fig. 10. A torque of 25 Nm was applied. Tensile strength tests were performed at the identical test speed and

equipment as previously described, cf. Fig. 10, until reaching specimens' failure. Load and crosshead displacement were recorded using TestXpert® software and the optical 2D/3D measuring system ARAMIS® was used to analyze full-field deformation of the surface during testing. To evaluate the CTRC specimens, an automated crack evaluation tool (ACE), as described in Ref. [5], was utilized. This tool automates the measurement of crack width, crack number, and crack distribution. Additionally, virtual extensometers can be added for strain analysis. In the analysis, the x-axis was aligned with the tensile direction, while the y-axis was oriented perpendicular to it.

4. Results and discussion

4.1. Experimental results of CTR

To evaluate the impact of freeze-thaw exposure on CTR, tensile strength tests of CTR-Ref and CTR-FT were examined and the results of tensile strength and Young's Modulus compared. The Young's Modulus was evaluated within the linear elastic range between 10 % and 60 % of the ultimate strain. The tensile strength results for the FT-conditioned materials indicated an average increase of 2 % compared to the reference series. Additionally, the evaluation of Young's Modulus showed a 1.2 % increase in stiffness for the FT-conditioned materials relative to the reference, cf. Fig. 14. These findings suggest that the FT temperature condition for 28 days has no significant impact on the mechanical properties of the materials. A weakening of the bond between impregnation material and carbon filaments, as reported in the literature based on tensile strength tests, could not be confirmed in the test results of the material investigated in this study [33].

Furthermore, no significant differences were determined in the percentual change in mass relative to the reference mass on the day of the FT cycle start, cf. Fig. 15. The observed increases in mass may be attributed to measurement inaccuracies of the scale. Based on the findings, it can be assumed that the material behavior of the CTR remains unaffected by thermal freeze-thaw condition over a 28-day period. This indicates that the FT-cycle does not have a significant adverse impact on the mechanical properties of the material.

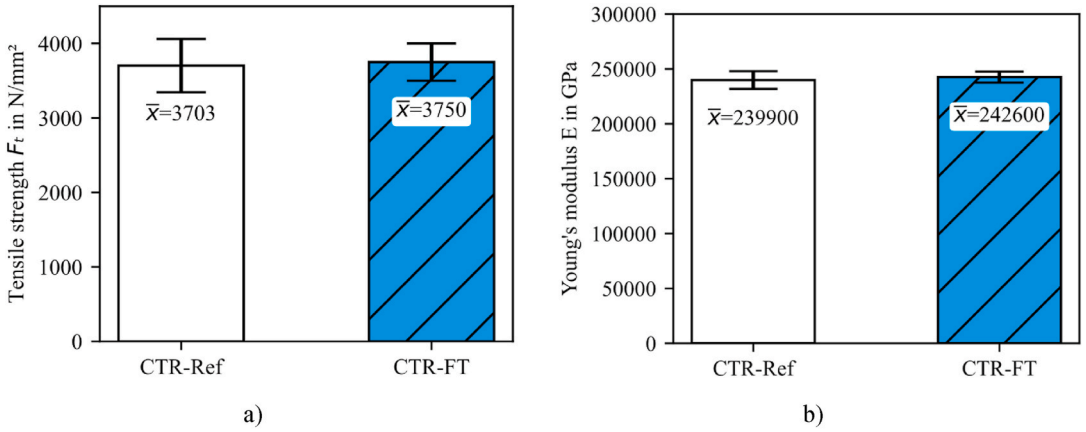

Fig. 14. Fiber strand tensile strength test results: a) Mean tensile strength values $\overline{X}$ with standard deviation; b) Mean Young's Modulus values $\overline{X}$ with standard deviation.

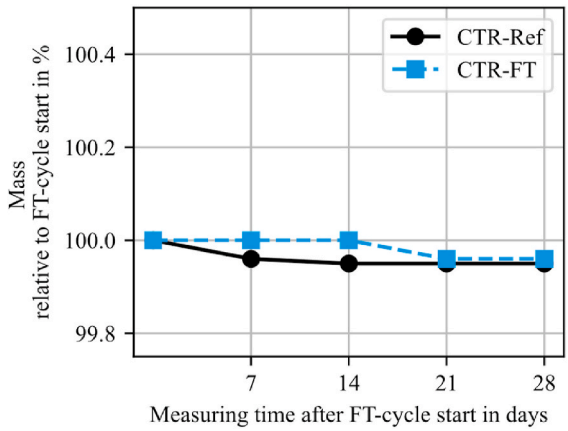

Fig. 15. Mass change of CTR.

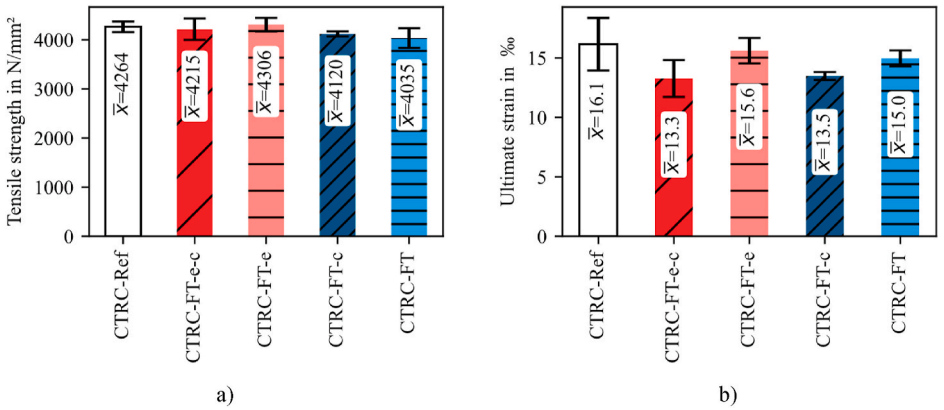

Fig. 16. Mean value $\overline{X}$ of tensile strength tests of CTRC uniaxial tensile specimen: a) Mean tensile strength values $\overline{X}$ with standard deviation; b) Ultimate strain values $\overline{X}$ with standard deviation.

4.2. Experimental results of CTRC

To evaluate the behavior of the composite material with electrically heated CTR under freeze-thaw cycling, tensile strength tests were examined on CTRC. The ultimate tensile strength and ultimate strain after freeze-thaw exposure were compared to those of CTRC-Ref.

The results indicated, that compared to CTRC-Ref, freeze-thaw exposure resulted in a maximum average deviation of 5 %. However, due to the standard deviations shown in Fig. 16, no clear trend could be observed. On average, the tensile strength of the electrically heated CTRC-FT-e-c and CTRC-FT-e series corresponds to the results of the CTRC-Ref series. In contrast, the tensile strength of the non-heated CTRC-FT-c and CTRC-FT series decreased by $\overline{X} = 4.4$ %. These results suggest that the electrical heating may have reduced the impact of freeze-thaw cycling, leading to tensile strengths comparable to the reference values.

Additionally, the analysis of the ultimate strain reveals that, on average, the ultimate strain for the non-heated series decreased by 12 % compared to CTRC-Ref. It was observed that the tensile strength of the pre-cracked series, CTRC-FT-e-c and CTRC-FT-c, was consistently lower compared to the uncracked series, CTRC-FT-e and CTRC-FT. This development was supported by the ultimate strain results. The authors assume that the pre-induced cracks facilitate the penetration of moisture into the specimens. This moisture absorption may lead to a more pronounced weakening of the composite matrix during freeze-thaw exposure. However, the results examined in Section 4.1 do not support the presence of embrittlement in the CTR in conjunction with a reduced Young's Modulus. Additionally, the impact of the RM-A4 layer on the CTR can be assessed by comparing the tensile strength results of the CTR (cf. Fig. 14, Section 4.1) and the CTRC (cf. Fig. 16). A higher tensile strength was observed in the CTRC compared to the CTR specimens. The authors suggest that the increased textile strength in the CTRC could be attributed to differences in the load application within the experimental setup, as well as variations in material batches. The material properties of CTR tensile strength, according to the manufacturer's specifications, is 12 % higher [25].

Furthermore, the results were compared to the summarized literature data, specifically represented by the reduction factor K_{FT}. The experimental results of this study showed no significant deviations compared to the literature data with coated CTR. The results of the unimpregnated CTR series by Refs. [16,18] showed $K_{FT} > 1.1$ after 50 freeze-thaw cycles, in comparison to the impregnated materials. Although similar numbers of freeze-thaw cycles were applied, the material combination with epoxy resin impregnated CTRC indicated a decreased strength compared to the results of Nobili et al. [18], cf. Fig. 17. The impregnation materials significantly influence the mechanical behavior of the reinforcements.

With the assistance of digital image correlation measurements and the evaluation tool ACE, crack width and crack distribution were analyzed for the investigated CTRC series. On average, the CTRC specimens without crack initiation exhibited increased crack widths of 20 % compared to the series with pre-induced cracks prior to freeze-thaw exposure, cf. Fig. 18. The crack widths of CTRC-FT-e and CTRC-FT indicated only minor differences, on average, compared to CTRC-Ref. The authors assume that during the unloading of the pre-cracked specimens, the cracks do not fully return to their original state. As a result, the initial gauge length of the specimens was extended. During the final tensile strength tests, the analysis was based on the reference length at the beginning of the tests. The indicated differences in crack width could be attributed to this phenomenon. This elongation of the gauge length after the first loading was evident in the results of the cyclic crack opening test presented by Morales [1].

This was further explained by comparing the crack widths at 2560 N/mm^2 (Stage IIb – finished crack pattern). The results for the pre-cracked series after 28 days were, on average, comparable to those observed during the initial loading after 63 days. The cracks that were reopened exhibit smaller crack widths, attributed to the previously described factors. The differences in crack width between the initial and second loading range from 0.02 mm to 0.03 mm, as shown in Fig. 18 a) and 18 b).

In addition, the findings revealed that the reduction in crack width due to crack initiation after 28 days was accompanied by an increase in the number of cracks compared to CTRC-Ref and the non-pre-cracked series, cf. Fig. 19. This phenomenon may be attributed to the timing of tensile strength test; at 28 days, the hydration process is less progressed than at 63 days. A softer mortar at

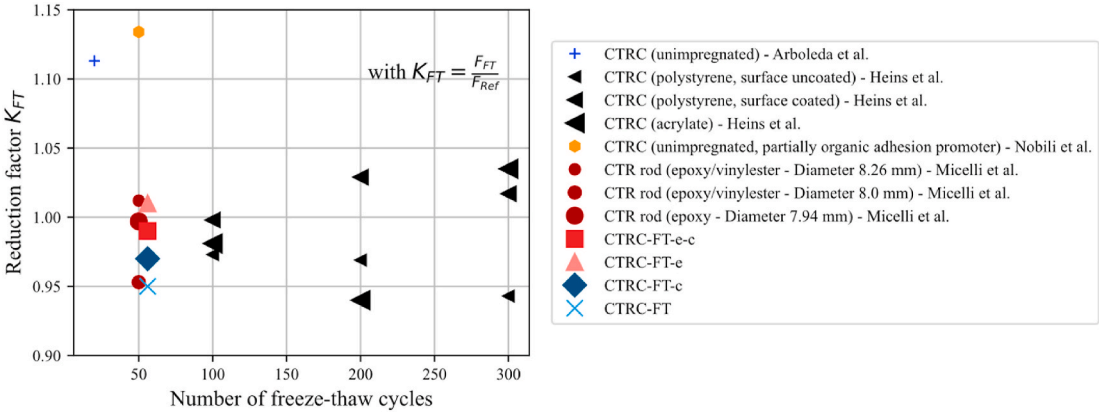

Fig. 17. Reduction factor K_{FT} related to the tensile strength of reference conditions [2,15,16,18].

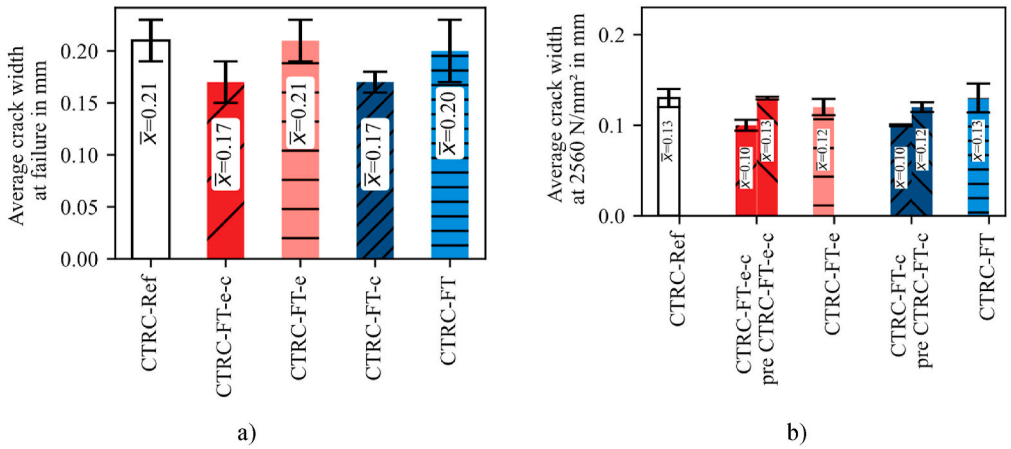

Fig. 18. Mean value $\overline{X}$ of crack width of CTRC uniaxial tensile specimen: a) Average crack width at failure values with standard deviation; b) Average crack width at 2560 N/mm^2 with standard deviation.

this stage would facilitate the formation of numerous small cracks. During the final tensile strength tests of the pre-cracked series, the pre-existing cracks were reopened, and no additional cracks form. This was also indicated in the tensile strength at initial crack, relative to the cross-sectional area of the uniaxial tensile specimen (20 × 60 mm^2), which confirmed the described differences. Due to

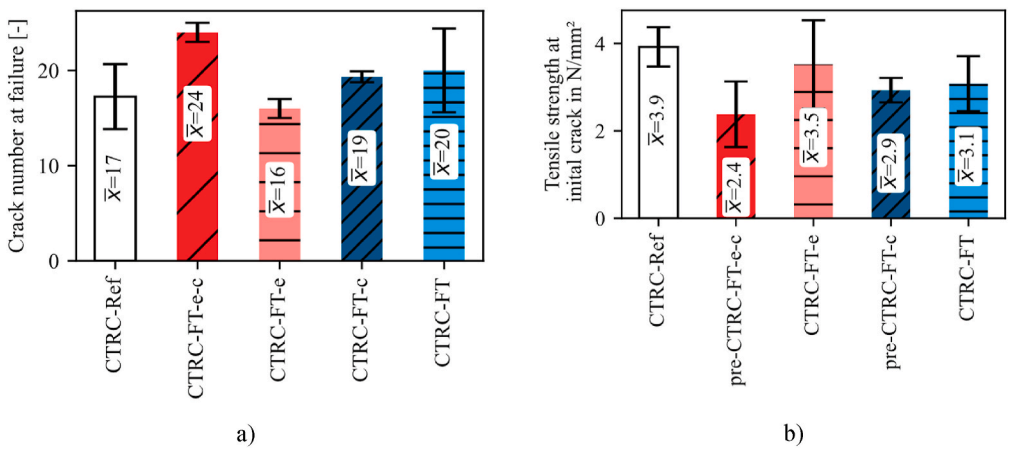

Fig. 19. Initial crack and crack number of CTRC uniaxial tensile specimen: a) Average crack number $\overline{X}$ at failure values with standard deviation; b) Mean value $\overline{X}$ of tensile strength at initial crack with standard deviation.

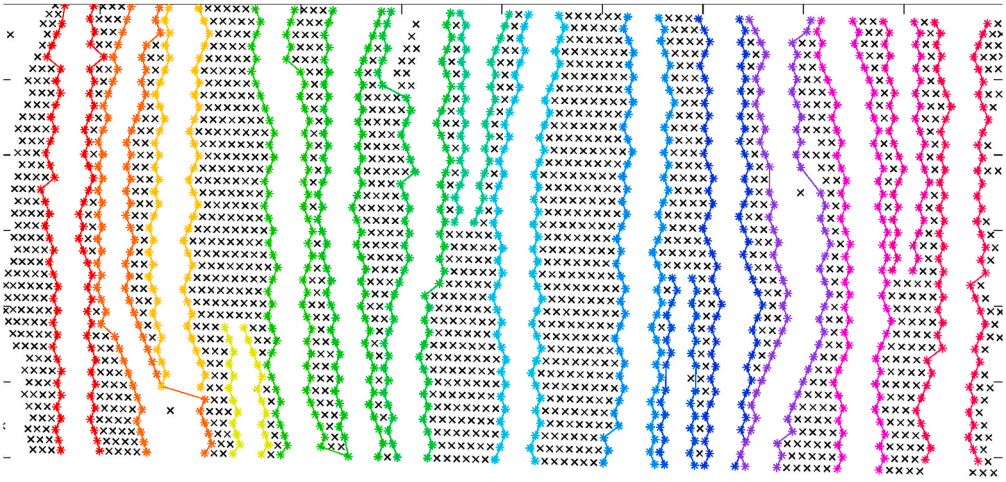

Fig. 20. Exemplary crack pattern of the investigated CTRC-FT-1 uniaxial tensile specimen immediately before failure.

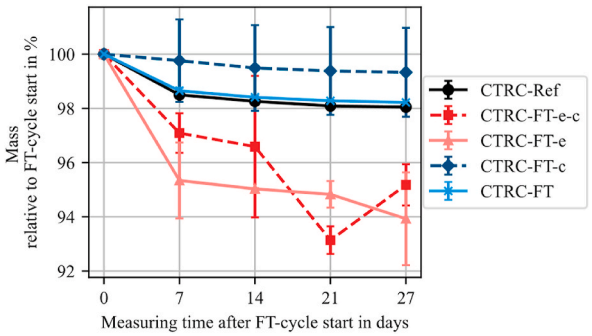

Fig. 21. Mass change of CTRC.

the degree of hydration, the tensile strength at initial crack at 28 days was reduced compared to the results at 63 days, leading to decreased pre-series values. Additionally, the average tensile strength at initial crack for the FT-series was reduced compared to those of CTRC-Ref, cf. Fig. 19 b).

Furthermore, no influence of the electrical heating on the average crack widths and crack distribution was observed. This suggests that the electrical carbon heating system does not negatively impact cracking behavior.

For further investigation, Fig. 20 depicts representative crack distribution immediately before failure for the CTRC uniaxial tensile specimens after freeze-thaw exposure. No significant influence on the crack pattern, such as irregular width across the cross-section or protrusions, was examined after freeze-thaw cycling. Consequently, if a crack occurs in the composite structure and is affected by electrical heating, the crack distribution is expected to remain typical. These results support the findings of Dahlhoff et al. [7] concerning higher electrical heating power up to 80 °C.

Additionally, the average mass change of the specimens was analyzed at 7-day intervals, compared to the reference. The results indicated an increased mass loss within the first 7 days. Subsequently, a gradual decrease of up to 6 % was observed, as shown in

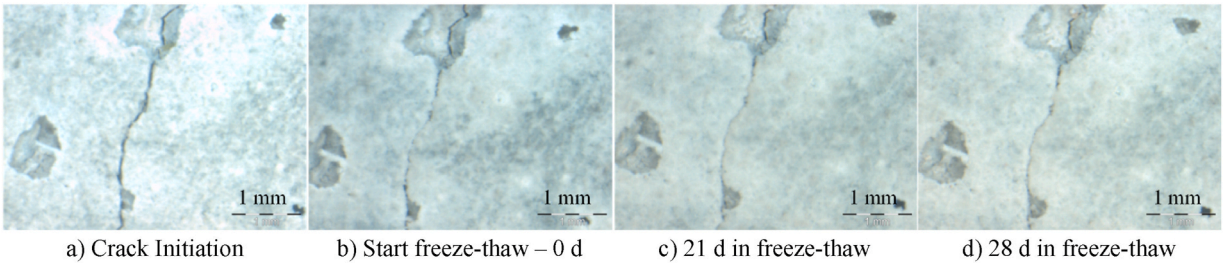

Fig. 22. Micrographs of pre-cracked concrete CTRC-FT-c-1b under freeze-thaw exposure: a) Initial crack; b) Starting freeze-thaw – 0 d; .c) Freeze-thaw for 21 days; d) Freeze-thaw for 28 days.

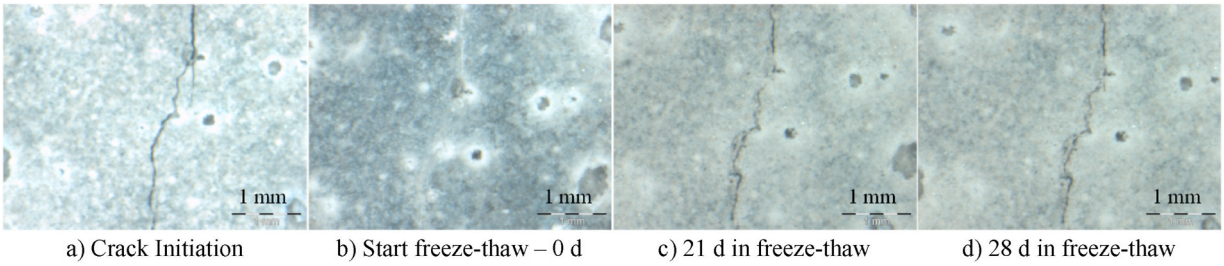

Fig. 23. Micrographs of pre-cracked concrete CTRC-FT-c-2b under freeze-thaw exposure: a) Initial crack; b) Starting freeze-thaw – 0 d; .c) Freeze-thaw for 21 days; d) Freeze-thaw for 28 days.

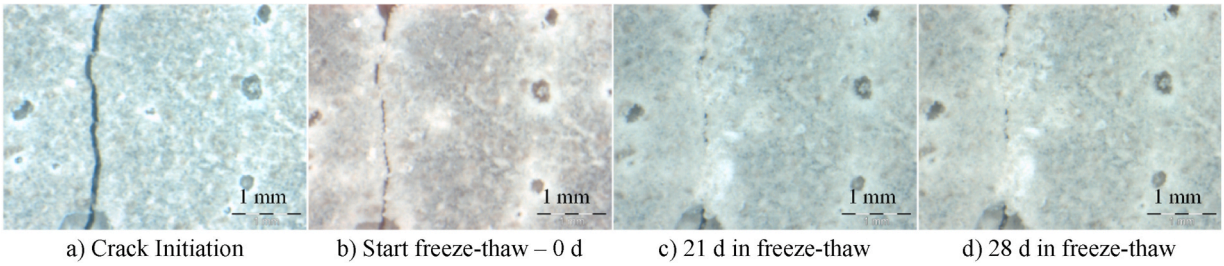

Fig. 24. Micrographs of pre-cracked concrete CTRC-FT-e-c-1a under freeze-thaw exposure: a) Initial crack; b) Starting freeze-thaw – 0 d; .c) Freeze-thaw for 21 days; d) Freeze-thaw for 28 days.

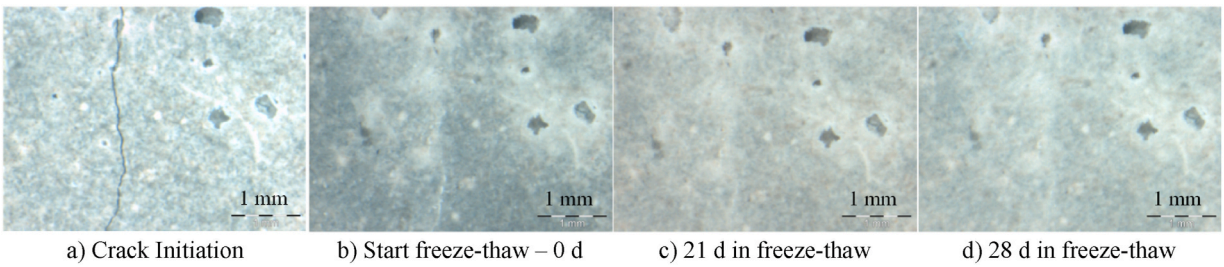

Fig. 25. Micrographs of pre-cracked concrete CTRC-FT-e-c-1b under freeze-thaw exposure: a) Initial crack; b) Starting freeze-thaw – 0 d; .c) Freeze-thaw for 21 days; d) Freeze-thaw for 28 days.

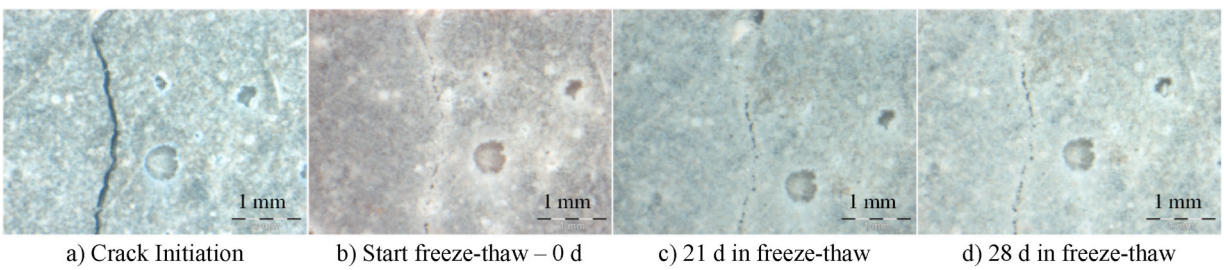

Fig. 26. Micrographs of pre-cracked concrete CTRC-FT-e-c-2a under freeze-thaw exposure: a) Initial crack; b) Starting freeze-thaw – 0 d; .c) Freeze-thaw for 21 days; d) Freeze-thaw for 28 days.

Fig. 21. Furthermore, the electrically heated specimens exhibit an increased mass loss compared to the non-heated series. The authors suggest that electrical heating reduces the condensation of water on the specimens, leading to an increased mass loss.

A total of eight cracks were examined, with two cracks each in two electrically heated specimens and two non-heated specimens for comparison. Figs. 22–26 summarize selected microscope images for the investigated time periods. The micrographs depict pre-cracked CTRC specimens at 16 × magnification, illustrating the crack initiation, the condition at the start of freeze-thaw cycles, and the progression after 21 and 28 days of freeze-thaw exposure. Microscopic analysis indicated that all cracks began to heal during the seven-day water storage following manufacturing (0d). This process was continued throughout the freeze-thaw cycles up to 28 days and is

exemplarily shown in Figs. 22–26, illustrating the results after 21 and 28 days.

Moreover, four of the cracks were closed completely during the water storage period (0d), while additionally three cracks were continued to heal during freeze-thaw cycling (28d). Furthermore, no significant differences were observed between 21 days and 28 days during the freeze-thaw cycling process. The healing is attributed to the formation of calcium carbonate crystals. Besides this healing, spalling along a crack was observed in only one of the eight cracks investigated. Since this occurrence was isolated, the spalling cannot be ascribed to electrical heating.

The development and healing of cracks do not show significant differences between heated and non-heated specimens, indicating comparable self-healing behavior in both types of series.

5. Conclusion and outlook

Within the framework of this investigation, the potential of ice-prevention using electrically heated carbon textile reinforcement in construction materials, as well as the impact of freeze-thaw exposure, was examined. Based on preliminary findings described, this investigation focused on the tensile strength of both CTR and the composite material CTRC. The research specifically investigated the tensile load-bearing behavior and crack performance under freeze-thaw environment.

The key findings of this study can be summarized as follows.

- Overall, the application of electrically heated CTR had shown significant potential in preventing the freezing of CTRC at sub-zero ambient temperatures. However, it is crucial to develop and optimize the appropriate clamping voltage for each material combination, with necessary adjustments for accommodate varying temperatures below 0 °C. The tensile strength tests revealed a decreased tensile strength after freeze-thaw exposure for test series without electrical heating, CTRC-FT-c and CTRC-FT. This can be attributed to the effectiveness of the heating functionality.
- For the roving component, freeze-thaw loading over the 28-day period did not show any detrimental effects on tensile strength or Youngs' modulus. The roving tensile strength tests did not indicate any embrittlement between the impregnation material and the carbon filaments. Furthermore, mass change measurements did not reveal any adverse trends in material properties.
- Moreover, the analysis of crack widths and crack distribution indicated no detrimental effects attributable to electrical heating. Additionally, crack healing was not adversely affected by the heating process. Should the heating principle have induced physical or chemical changes due to temperature fluctuations, no adverse impacts were detected within the temperature profile applied. Given that the CTRC is intended to remain frost-free, temperatures capable of causing damage to the reinforcement were not expected. Furthermore, it was determined that the 28-day freeze-thaw exposure had no detrimental effect on the average crack width of the CTRC at failure.
- Furthermore, the findings indicated that the application of electrical heating resulted in a more pronounced mass loss of the specimens during the investigation period. These results suggest that electrically heated CTRC may accelerate hydration after production and could potentially reduce water penetration into the structure over prolonged use by facilitating improved moisture evaporation.

These results are of fundamental importance as they highlight the possibility to use electrically heated CTRC in building components. They enable a precise quantification of the material properties influenced by electrical heating, thereby improving the understanding and expanding the potential applications of this innovative material within the construction sector.

Further investigation should focus on the application and monitoring of electrically heated carbon concrete in structural components, for example bridges. For this purpose, additional material combinations of CTR and concrete should be characterized. Subsequent studies could determine material-specific parameters, further analyzing the proposed crack healing mechanism, and generate mathematical models to predict the temperature development of electrically heated CTRC structures. Moreover, long-term effects of electrical heating on potential damage to the CTR, as well as the concrete and the composite behavior should be investigated. The proposed further investigation can be integrated into the research project MultiTexBridge, grant number KK5038622KT4, funded by BMWK.

CRediT authorship contribution statement

Annette Dahlhoff: Writing – review & editing, Writing – original draft, Visualization, Validation, Supervision, Software, Resources, Project administration, Methodology, Investigation, Formal analysis, Data curation, Conceptualization. **Michael Raupach:** Writing – review & editing, Supervision, Project administration.

Funding

This research did not receive any specific grant from funding agencies in the public, commercial, or not-for-profit sectors.

Declaration of competing interest

The authors declare that they have no known competing financial interests or personal relationships that could have appeared to influence the work reported in this paper.

Data availability

The experimental data used to support the findings of this research work are included in the article.

References

[1] C. Morales Cruz, Crack-distributing Carbon Textile Reinforced Concrete Protection Layers, RWTH Aachen University, Aachen, Germany, 2020. Ph.D. Thesis.
[2] K. Heins, M. Kimm, L. Olbrueck, M. May, T. Gries, A. Kolkmann, G.-S. Ryu, G.-H. Ahn, H.-Y. Kim, Long-term bonding and tensile strengths of carbon textile reinforced mortar, Materials 13 (20) (2020) 4485, https://doi.org/10.3390/ma13204485.
[3] A. Dahlhoff, C. Morales Cruz, M. Raupach, Influence of selected impregnation materials on the tensile strength for carbon textile reinforced concrete at elevated temperatures, Buildings 12 (12) (2022) 2177, https://doi.org/10.3390/buildings12122177.
[4] A. Asgharzadeh, *Durability Of Polymer Impregnated Carbon Textiles as CP Anode for Reinforced Concrete* Dissertation, Rheinisch-Westfälische Technische Hochschule Aachen, 2019.
[5] A. Dahlhoff, M. Raupach, Crack analysis of textile reinforced concrete using automated crack evaluation via digital image correlation, Buildings 13 (12) (2023) 2984, https://doi.org/10.3390/buildings13122984.
[6] M.S.F. Tröger, M.S.S. Große, M.E.D.-I.T. Rudloff, I.T. Heimbold, *Entwicklung einer elektrischen Kontaktierung für multifunktionale Carbonfaser-Strukturen in Beton* 19, AALE-Konferenz, Luxemburg, 2023, 08.03.-10.03.2023.
[7] A. Dahlhoff, M. Raupach, Electrical heating of carbon textile reinforced concrete — possible effects on tensile load-bearing behavior, Appl. Sci. 14 (11) (2024) 4430, https://doi.org/10.3390/app14114430.
[8] J. Schöffel, N. Abdelkaf, Rethinking construction: the market for heatable carbon concrete building components. Fraunhofer-Zentrum für Internationales Management und Wissensökonomie IMW Jahresbericht 2018, 2019, pp. 66–67.
[9] C³InteF – Integration der Heizfunktion in Bauelementen aus Carbonbeton. https://www.imw.fraunhofer.de/de/forschung/unternehmensentwicklung/geschaeftsmodelle/projekte/c-intef.html. (Accessed 25 February 2024).
[10] Load-bearing concrete members with adaptive heating structures made of carbon fibres for buildings with climate neutral energy strategy. https://tu-dresden.de/bu/bauingenieurwesen/imb/forschung/Forschungsfelder/CRC/fue-crc/FuE_finished/smarttex?set_language=en. (Accessed 25 February 2024).
[11] M. Frenzel, M. Stelzmann, A. Söhnchen, Cube – demonstration areas and exhibition objects, Beton-und Stahlbetonbau 118 (2023) 133–139, https://doi.org/10.1002/best.202300010.
[12] H. Abdualla, H. Ceylan, S. Kim, K. Gopalakrishnan, P.C. Taylor, Y. Turkan, System requirements for electrically conductive concrete heated pavements, Transp. Res. Rec. 2569 (1) (2016) 70–79, https://doi.org/10.3141/2569-08.
[13] Y. Liu, Y. Lai, D. Ma, Melting snow on airport cement concrete pavement with carbon fibre heating wires, Mater. Res. Innov. 19 (2015) S10–S95, https://doi.org/10.1179/1432891715Z.0000000002097.
[14] S. Xu, W. Yu, S. Song, Numerical simulation and experimental study on electrothermal properties of carbon/glass fiber hybrid textile reinforced concrete, Sci. China Technol. Sci. 54 (2011) 2421–2428, https://doi.org/10.1007/s11431-011-4503-0.
[15] F. Micelli, A. Nanni, Durability of FRP rods for concrete structures, Constr. Build. Mater. 18 (7) (2004) 491–503, https://doi.org/10.1016/j.conbuildmat.2004.04.012.
[16] D. Arboleda, S. Babaeidarabad, C. Hays, A. Nanni, G. Fisher, E. Scholar, Durability of fabric reinforced cementitious matrix (FRCM) composites, in: 7th International Conference of FRP Composites in Civil Engineering (CICE 2014), Vancouver, BC, Canada, 2014, 20–22 August 2014.
[17] S. Yin, Y. Li, Z.-y. Jin, P.-h. Li, Interfacial properties of textile-reinforced concrete and concrete in chloride freezing-and-thawing cycle, ACI Mater. J. (2018), https://doi.org/10.14359/51701919, 115-M18.
[18] A. Nobili, C. Signorini, On the effect of curing time and environmental exposure on impregnated Carbon Fabric Reinforced Cementitious Matrix (CFRCM) composite with design considerations, Compos. B Eng. 112 (2017) 300–313, https://doi.org/10.1016/j.compositesb.2016.12.022.
[19] C. Tedeschi, S. Perego, M.R. Valluzzi, Study on local effects of aggressive environmental conditions on masonry strengthened with FRCM, in: 16th International Brick and Block Masonry Conference, Padova, Italy, 2016, 26-30 June 2016.
[20] J. Sheng, L.-c. Wang, S.-p. Yin, Study on the mechanical performance of TRC-strengthened RC beams under a salt freeze–thaw environment, Cold Reg. Sci. Technol. 192 (2021) 103384, https://doi.org/10.1016/j.coldregions.2021.103384.
[21] Y. Shiping, F. Linli, Z. Junling, Study on the tensile and flexural mechanical properties of TRE in freezing-thawing environments, Constr. Build. Mater. 268 (2021) 121150, https://doi.org/10.1016/j.conbuildmat.2020.121150.
[22] M. Alma'aitah, B. Ghiassi, A. Dalalbashi, Durability of textile reinforced concrete: existing knowledge and current gaps, Appl. Sci. 11 (6) (2021) 2771. https://www.mdpi.com/2076-3417/11/6/2771.
[23] TR IH, Technische Regel - Instandhaltung von Betonbauwerken (TR Instandhaltung) - Teil 1: Anwendungsbereich und Planung der Instandhaltung, Deutsches Institut für Bautechnik (DIBt), 2020.
[24] TR IH, Technische Regel - Instandhaltung von Betonbauwerken (TR Instandhaltung) - Teil 2: Merkmale von Produkten oder Systemen für die Instand-setzung und Regelungen für deren Verwendung, Deutsches Institut für Bautechnik (DIBt), 2020.
[25] Technical Product Data Sheet - solidian Retrieved 12.December.2024 from https://www.solidian-kelteks.com/en/products/construction/reinforcements/meshes/rigid-meshes/anticrack-detail.
[26] Sto SE & Co, KGaA: Leistungserklärung für das Bauprodukt StoCrete TS 203, Retrieved, https://www.sto.de/s/p/a1F2p00000NwG6bEAF/stocrete-ts-203, 2022. (Accessed 2 October 2024).
[27] M. Lenting, Untersuchungen zu mineralischen Tränkungen von technischen Textilien für die flächige Instandsetzung von gerissenen Bauwerken mit Textilbeton, Technische Universität Dortmund, Germany, 2023. Ph.D. Thesis.
[28] E. Schütze, J. Bielak, S. Scheerer, J. Hegger, M. Curbach, Uniaxial tensile test for carbon reinforced concrete with textile reinforcement, Beton- Stahlbetonbau 113 (2018) 33–47, https://doi.org/10.1002/best.201700074.
[29] DIN EN 1015-3: Methods of test for mortar for masonry - Part 3: determination of consistence of fresh mortar (by flow table); German version EN 1015-3:1999+A1:2004+A2:2006. (2007-05). In: DIN Deutsches Institut für Normung e. V.
[30] DIN EN 1015-6: Methods of test for mortar for masonry - Part 6: determination of bulk density of fresh mortar; German version EN 1015-6:1998+A1:2006. (2007-05). In: DIN Deutsches Institut für Normung e. V.
[31] DIN EN 1015-7: Methods of test for mortar for masonry - Part 7: determination of air content of fresh mortar; German version EN 1015-7:1998. (1998-12). In: DIN Deutsches Institut für Normung e. V.
[32] DIN EN 1015-11: Methods of test for mortar for masonry - Part 11: determination of flexural and compressive strength of hardened mortar; German version EN 1015-11:2019. (2020-01). In: DIN Deutsches Institut für Normung e. V.
[33] J.-W. Shi, H. Zhu, G. Wu, Z.-S. Wu, Tensile behavior of FRP and hybrid FRP sheets in freeze–thaw cycling environments, Compos. B Eng. 60 (2014) 239–247, https://doi.org/10.1016/j.compositesb.2013.11.026.